

Mononuclear Clusterfullerene Single-Molecule Magnet Containing Strained Fused-Pentagons Stabilized by a Nearly Linear Metal Cyanide Cluster

Fupin Liu⁺, Song Wang⁺, Cong-Li Gao, Qingming Deng, Xianjun Zhu, Aram Kostanyan, Rasmus Westerström, Fei Jin, Su-Yuan Xie,^{*} Alexey A. Popov,^{*} Thomas Greber,^{*} and Shangfeng Yang^{*}

Abstract: Fused-pentagons results in an increase of local steric strain according to the isolated pentagon rule (IPR), and for all reported non-IPR clusterfullerenes multiple (two or three) metals are required to stabilize the strained fused-pentagons, making it difficult to access the single-atom properties. Herein, we report the syntheses and isolations of novel non-IPR mononuclear clusterfullerenes $MNC@C_{76}$ ($M = Tb, Y$), in which one pair of strained fused-pentagon is stabilized by a mononuclear cluster. The molecular structures of $MNC@C_{76}$ ($M = Tb, Y$) were determined unambiguously by single-crystal X-ray diffraction, featuring a non-IPR $C_{2v}(I9138)-C_{76}$ cage entrapping a nearly linear MNC cluster, which is remarkably different from the triangular MNC cluster within the reported analogous clusterfullerenes based on IPR-obeying C_{82} cages. The $TbNC@C_{76}$ molecule is found to be a field-induced single-molecule magnet (SMM).

Fullerenes are closed carbon cages with hollow interiors, and such unique structures bring about intriguing physical and chemical properties.^[1] Most fullerenes isolated during the past three decades are based on classical carbon cages composed of hexagons and pentagons only,^[1,2] for which the stability is generally determined by the isolated pentagon rule (IPR) proposed by Kroto in the 1980s.^[3] According to IPR, fused-pentagons result in an increase of local steric strain of a carbon cage, thus destabilizing the fullerene.^[3,4] Stabilization of the strained fused-pentagon within a non-IPR fullerene cage has been fulfilled by either endohedral or

exohedral derivatization.^[4] In particular, for endohedral fullerenes which are a special class of fullerene with an atom, ion, or cluster entrapped in the interior of carbon cage,^[5] the strong coordination of the entrapped metal ion(s) with the fused-pentagon gives rise to an intramolecular electron transfer and consequently stabilization of the non-IPR endohedral fullerene.^[4-6] Most of the non-IPR endohedral fullerenes reported to date are based on clusterfullerenes^[7] owing to the feasibility of entrapping multiple metals in diverse forms of metal clusters, such as $Sc_3N@C_{68}$,^[6a,b] $Gd_3N@C_{2n}$ ($2n = 78, 82, 84$),^[6c-e] $LaSc_2N@C_{80}$,^[6f] and $Sc_2S@C_{72}$.^[6g] Noteworthy, for these reported non-IPR clusterfullerenes, multiple (two or three) metal ions are required to stabilize simultaneously the charged metal clusters and the fused-pentagons. Hence, it is desirable to synthesize novel non-IPR endohedral fullerenes containing mononuclear metal clusters.

Clusterfullerenes have been recently recognized as single molecule magnets (SMMs) with potential applications in spintronics, quantum computing, and high-density storage devices.^[8,9] To date only a few endohedral fullerene SMMs have been reported, including $Ln_xSc_{3-x}N@C_{80}$ ($Ln = Dy, Ho, x = 1, 2$)^[9a-d] and $Dy_2TiC@C_{80}$,^[9e] which are all based on an I_h-C_{80} cage entrapping multiple rare-earth-metal ions that are fixed as a triangle along with the central non-magnetic ion (N or C). For such clusterfullerene SMMs based on multiple metal centers, their magnetic properties are generally determined jointly by the entrapped individual paramagnetic

[*] Dr. F. P. Liu,^[+] Dr. S. Wang,^[+] X. J. Zhu, F. Jin, Prof. Dr. S. F. Yang Hefei National Laboratory for Physical Sciences at Microscale, CAS Key Laboratory of Materials for Energy Conversion, Department of Materials Science and Engineering, Synergetic Innovation Center of Quantum Information & Quantum Physics, University of Science and Technology of China Hefei 230026 (China)
E-mail: sfyang@ustc.edu.cn

Dr. C.-L. Gao, Prof. Dr. S.-Y. Xie State Key Laboratory of Physical Chemistry of Solid Surfaces and Department of Chemistry, iChEM (Collaborative Innovation Center of Chemistry for Energy Materials), College of Chemistry and Chemical Engineering, Xiamen University Xiamen 361005 (China)
E-mail: syxie@xmu.edu.cn

Dr. Q. M. Deng, Dr. A. A. Popov Leibniz Institute for Solid State and Materials Research Dresden Helmholtzstrasse 20, Dresden 01069 (Germany)

E-mail: a.popov@ifw-dresden.de

A. Kostanyan, Dr. R. Westerström, Prof. Dr. T. Greber Physik-Institut, Universität Zürich Winterthurerstrasse 190, 8057 Zürich (Switzerland)
E-mail: greber@physik.uzh.ch

[+] These authors contributed equally to this work.

Supporting information and the ORCID identification number(s) for the author(s) of this article can be found under <http://dx.doi.org/10.1002/anie.201611345>.

© 2017 The Authors. Published by Wiley-VCH Verlag GmbH & Co. KGaA. This is an open access article under the terms of the Creative Commons Attribution Non-Commercial NoDerivs License, which permits use and distribution in any medium, provided the original work is properly cited, the use is non-commercial, and no modifications or adaptations are made.

constituents, making it difficult to access the single-atom properties. Very recently we reported new SMMs based on terbium cyanide clusterfullerenes TbNC@C_{82} , which provide a model system for the study of endohedral fullerene SMM owing to its structural simplicity resulted from the mononuclear nature.^[10a] Thus, it is highly desirable to synthesize new mononuclear clusterfullerene SMMs based on other carbon cages.

Herein we report novel non-IPR mononuclear clusterfullerene SMM containing one pair of fused-pentagons, which is stabilized by a mononuclear cyanide cluster. Two C_{76} -based mononuclear cyanide clusterfullerenes MNC@C_{76} ($M = \text{Tb, Y}$) are synthesized and isolated, and their molecular structures are determined unambiguously by single-crystal X-ray diffraction, revealing the non-IPR feature of the C_{76} cage as well as the geometry of the entrapped MNC cluster. The electronic and magnetic properties of MNC@C_{76} are further characterized, and TbNC@C_{76} molecule is identified as a field-induced SMM.

MNC@C_{76} ($M = \text{Tb, Y}$) were synthesized by a modified Krätschmer–Huffman DC arc discharge method using a mixture of Tb_4O_7 (or Y_2O_3) and graphite (molar ratio of $M:C = 1:15$) as the raw material under 400 mbar He and 10 mbar N_2 gas.^[10] Isolations of MNC@C_{76} ($M = \text{Tb, Y}$) were performed by multi-step HPLC (see Supporting Information for experimental details). The high purities of MNC@C_{76} ($M = \text{Tb, Y}$) were confirmed by laser desorption time-of-flight (LD-TOF) mass spectroscopic analyses (see Supporting Information Figure S4 and S6).

High quality cocrystals of MNC@C_{76} ($M = \text{Tb, Y}$) with $\text{Ni}^{\text{II}}(\text{OEP})$ ($\text{OEP} = \text{octaethylporphyrin}$), $\text{MNC@C}_{76} \cdot \text{Ni}(\text{OEP}) \cdot 2\text{C}_6\text{H}_6$, were obtained by layering a benzene solution of $\text{Ni}^{\text{II}}(\text{OEP})$ over the solution of MNC@C_{76} in benzene (for TbNC@C_{76}) or carbon disulfide (for YNC@C_{76}),^[6b–g, 10, 11] and were used for the X-ray crystallographic study. Figure 1 a,d show the relative orientations of MNC@C_{76} and $\text{Ni}^{\text{II}}(\text{OEP})$

molecules in $\text{MNC@C}_{76} \cdot \text{Ni}(\text{OEP}) \cdot 2(\text{C}_6\text{H}_6)$ cocrystals. For both cases of TbNC@C_{76} and YNC@C_{76} , the C_{76} cage is fully ordered, enabling the unambiguous determination of the carbon cage framework. However, the entrapped MNC cluster is disordered (see Supporting Information Figures S7–S8). For clarity, only the major site of the cluster was shown in Figure 1. The asymmetric unit of $\text{MNC@C}_{2v}(19138)\text{-C}_{76} \cdot \text{Ni}^{\text{II}}(\text{OEP}) \cdot 2(\text{C}_6\text{H}_6)$ has no crystallographic imposed symmetry and contains an intact fullerene molecule together with an intact $\text{Ni}^{\text{II}}(\text{OEP})$ molecule and two solvent benzene molecules (Figure 1 a,d). A remarkable structural feature of both cages of TbNC@C_{76} and YNC@C_{76} is that there is one pair of fused-pentagon within the same $C_{2v}(19138)\text{-C}_{76}$ cage (see Figure 1 b,e), thus violating IPR.^[2–4] Hence, $\text{MNC@C}_{2v}(19138)\text{-C}_{76}$ ($M = \text{Tb, Y}$) represents novel non-IPR mononuclear clusterfullerenes.

Quite similar to the cases of other reported clusterfullerenes including $\text{YNC@C}_s(6)\text{-C}_{82}$ and TbNC@C_{82} mononuclear cyanide clusterfullerenes,^[10] the entrapped TbNC/YNC clusters within $\text{TbNC@C}_{2v}(19138)\text{-C}_{76}$ and $\text{YNC@C}_{2v}(19138)\text{-C}_{76}$ both exhibit disorders. In fact, as many as 7 and 5 metal sites are refined for $\text{TbNC@C}_{2v}(19138)\text{-C}_{76}$ and $\text{YNC@C}_{2v}(19138)\text{-C}_{76}$, respectively (see Supporting Information Figures S7–S8). Among them, the major metal site has an occupancy of 0.689(3) and 0.871(2) for Tb and Y, respectively, which locates just under the junction of the fused-pentagon (see Figure 1 c,f). This is quite similar to the reported non-IPR clusterfullerenes such as $\text{Sc}_3\text{N@D}_3(6140)\text{-C}_{68}$ ^[6b] and $\text{Sc}_2\text{S@C}_s(10528)\text{-C}_{72}$.^[6g] Thus, it is the strong coordination interaction between Tb/Y metal and the cage that stabilizes the fused-pentagon within the non-IPR $C_{2v}(19138)\text{-C}_{76}$ cage.

For the reported $\text{YNC@C}_s(6)\text{-C}_{82}$ and $\text{TbNC@C}_{2v}(5)\text{-C}_{82}$ mononuclear cyanide clusterfullerenes, the entrapped MNC clusters both take a triangular geometry, and it is difficult to distinguish N and C atoms crystallographically because of their similarities on the atomic size and scattering power.^[10, 11d] However, for the present case of $\text{MNC@C}_{2v}(19138)\text{-C}_{76}$, N and C atoms within MNC cluster can be distinguished by combining the crystallographic data with DFT computational results. Our DFT computations of MNC@C_{76} ($M = \text{Tb, Y}$) reveal that, for the non-IPR cage isomers (C_{2v} , C_1 , C_s) of C_{76} , nearly linear (slightly V-shaped) M–N–C coordination is always preferred with the energy being 15–18 kJ mol^{-1} lower than that for linear M–C–N coordination. This agrees well with the M–N–C bond angle ($154.9(13)^\circ$ and $160.4(7)^\circ$ for Tb and Y, respectively, see Figure 1 c, f) determined by X-ray crystallography (see Supporting Information S4 for details). Hence, except for the non-IPR feature of the C_{76} cage, the nearly linear M–N–C configuration of the entrapped MNC cluster within MNC@C_{76} highlights another remarkable difference with the triangular geometry of the MNC cluster for the analogous clusterfullerenes based on IPR-obeying C_{82} cages, $\text{YNC@C}_s(6)\text{-C}_{82}$ and TbNC@C_{82} .^[10] A plausible explanation is that for non-IPR MNC@C_{76} a stronger M–cage interaction is required to stabilize the fused-pentagon as confirmed by the smaller distance of the shortest M–cage contact (see Figure S9 and Table S4), thus the coordination bonding between the metal atom and $[\text{NC}]^-$ ligand is weakened via the change of the bidentate $[\text{NC}]^-$ ligand (for the triangular MNC cluster

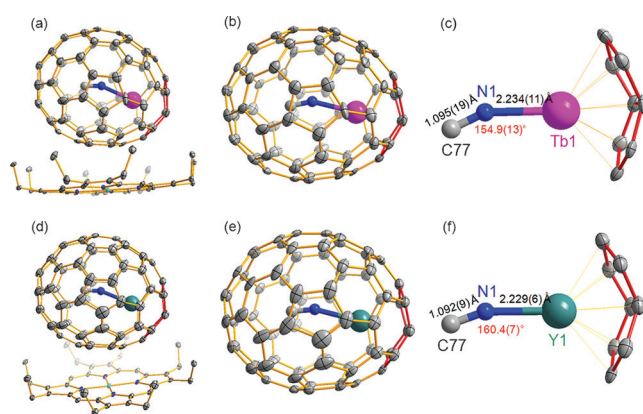


Figure 1. Single-crystal X-ray structures of $\text{TbNC@C}_{2v}(19138)\text{-C}_{76}$ (a,b) and $\text{YNC@C}_{2v}(19138)\text{-C}_{76}$ (d,e) shown with only the major Tb/Y (Tb1/Y1) positions.^[14] The fused-pentagon pair is highlighted in red. The structures of the major TbNC (c) and YNC (f) clusters within $C_{2v}(19138)\text{-C}_{76}$ cage with X-ray determined bond lengths, bond angles, and the interactions of the Tb/Y atom with the closest portions of the cage are also shown. Solvent molecules, hydrogen atoms and minor metal positions are omitted for clarity. Purple Tb; cyan Y; blue N; gray C; green Ni.

within $\text{MNC}@C_{82}$) to a monodentate one (for the nearly linear MNC cluster within $\text{MNC}@C_{76}$).

Such a dramatic geometric change of the entrapped TbNC cluster upon changing the carbon cage from IPR-obeying C_{82} to non-IPR C_{76} is further confirmed in terms of the N–C bond length. Interestingly, while the X-ray determined N–C bond length for $\text{YNC}@C_s(6)-C_{82}$ and $\text{TbNC}@C_{82}$ is in the range 0.935(11) to 1.05(4) Å,^[10] it elongates to 1.095(19) and 1.092(9) Å for $\text{TbNC}@C_{2v}(19138)-C_{76}$ and $\text{YNC}@C_{2v}(19138)-C_{76}$, respectively (see Figure 1c,f). These values are approaching those of the reported N–C triple bonds in traditional cyanide/nitrile compounds and cyano coordination complexes (1.12–1.17 Å).^[12] Thus, it is reasonable to assign the N–C bond within $\text{MNC}@C_{2v}(19138)-C_{76}$ as a triple bond, which appears to be compressed within $\text{MNC}@C_{82}$ despite of the larger cage size. This phenomenon is somewhat surprising if simply considering the cage-size effect, and can be interpreted by the weakened M–[NC][−] coordination bonding induced by the stronger M–cage interaction, which is required to stabilize the fused-pentagon of the non-IPR C_{76} cage as discussed above.

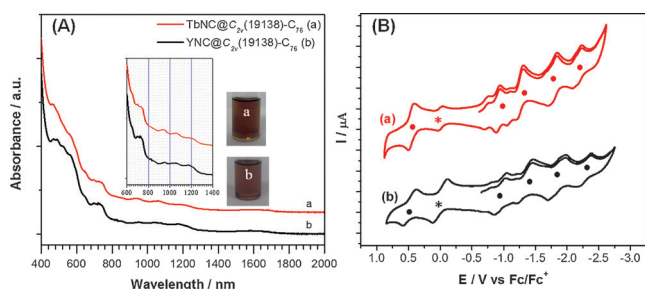


Figure 2. A) UV/Vis-NIR spectra of $\text{TbNC}@C_{2v}(19138)-C_{76}$ (a) and $\text{YNC}@C_{2v}(19138)-C_{76}$ (b) dissolved in CS_2 . Insets: Enlarged spectral region (600–1400 nm) and the photographs of samples in CS_2 . B) Cyclic voltammograms of $\text{TbNC}@C_{2v}(19138)-C_{76}$ (a) and $\text{YNC}@C_{2v}(19138)-C_{76}$ (b) in *o*-DCB solution. Ferrocene (Fc) was added as the internal standard and all potentials are referenced to the Fc/Fc^+ couple, TBAPF_6 as supporting electrolyte, scan rate: 100 mV s^{-1} . The half-wave potential ($E_{1/2}$) of each redox step is marked with a solid dot to aid comparison. The asterisk labels the oxidation peak of Fc.

Figure 2A shows the UV/Vis-NIR absorption spectra of $\text{TbNC}@C_{2v}(19138)-C_{76}$ and $\text{YNC}@C_{2v}(19138)-C_{76}$ dissolved in carbon disulfide (CS_2), and their characteristic absorption data are summarized in Table S6. Interestingly, their overall absorption spectra, the characteristic absorption peaks, the optical band-gap ($\Delta E_{\text{gap,optical}}$) and color of CS_2 solutions are almost identical, confirming their identity on the cage isomeric structure which predominantly determines the electronic absorption of endohedral fullerene with the same type of entrapped species.^[5,6]

The electronic properties of $\text{TbNC}@C_{2v}(19138)-C_{76}$ and

$\text{YNC}@C_{2v}(19138)-C_{76}$ are further investigated by cyclic voltammetry. Figure 2B shows their cyclic voltammograms measured in *o*-dichlorobenzene (*o*-DCB) with tetrabutylammonium hexafluorophosphate (TBAPF_6) as supporting electrolyte (see also Figures S14–S15), and their characteristic redox potentials are summarized in Table 1, which includes also those of other analogous C_{82} - and C_{76} -based endohedral fullerenes for comparison. Again, the characteristic redox potentials and the electrochemical gaps ($\Delta E_{\text{gap,ec}}$) of $\text{TbNC}@C_{2v}(19138)-C_{76}$ and $\text{YNC}@C_{2v}(19138)-C_{76}$ are almost identical (with the difference being less than 0.05 V, see Table 1), confirming further the decisive role of the carbon cage on the electronic properties of endohedral fullerenes with the same type of entrapped species.^[5,6] $\text{MNC}@C_{2v}(19138)-C_{76}$ show a larger separation between the second and third reduction steps (0.52 and 0.50 V for $\text{TbNC}@C_{76}$ and $\text{YNC}@C_{76}$, respectively) than those between the first two reduction steps (first-second, 0.35–0.38 V) and the last two reduction steps (third-fourth, 0.41–0.42 V), and this phenomenon is similar to the cases of $\text{YNC}@C_s(6)-C_{82}$ and $\text{TbNC}@C_{82}$ ($C_s(6)$, $C_2(5)$, $C_{2v}(9)$).^[10] Such a resemblance on the electrochemical behavior between $\text{MNC}@C_{2v}(19138)-C_{76}$ and $\text{MNC}@C_{82}$ suggests that they adopt the same electronic configuration, namely $[\text{M}^{3+}(\text{NC})^{-}]^{2+} @ [\text{C}_{2n}]^{2-}$, resulting in a closed-shell electronic configuration with non-degenerate low-lying LUMO and accessible LUMO + 1 orbitals.^[5,6,10,13a]

While $\text{YNC}@C_{76}$ is diamagnetic since there is no unpaired electron for the Y^{3+} cation, Tb^{3+} has eight 4f electrons with a 7F_6 Hund ground state, indicating that $\text{TbNC}@C_{76}$ is paramagnetic. We then studied the magnetic properties of $\text{TbNC}@C_{76}$ with a superconducting quantum interference device (SQUID). Figure 3A shows the normalized magnetizations of $\text{TbNC}@C_{76}$ versus the applied field-temperature quotient $x = \mu_0 H/T$ measured at seven temperatures between 1.8 and 10 K. The good scaling in this temperature range indicates that the ligand field, which splits the Hund ground state, is so strong that the low temperature magnetization may be described with one J_z level. Based on a perfect fit between the experimental magnetization data and the non-collinear magnetic moment model proposed previously for $\text{Dy}_x\text{Sc}_{3-x}\text{N}@C_{80}$,^[9a-c] the magnetic moment $|\mu|$ of $\text{TbNC}@C_{76}$ is determined to be $8.9 \mu_B$, which agrees well with the theoretical limit of $9 \mu_B$. Therefore, the Tb ground state is assigned to be $J_z = \pm 6$ (see Supporting Information S7). Such a large J_z value is a prerequisite for SMM.^[10a]

Table 1: Redox Potentials (V vs. Fc/Fc^+), electrochemical gaps ($\Delta E_{\text{gap,ec}}$) of $\text{MNC}@C_{2v}(19138)-C_{76}$ and other reported C_{82} - and C_{76} -based endohedral fullerenes.

Sample	$E_{1/2}$ [V vs. Fc/Fc^+]				E_{ox} 1st	$\Delta E_{\text{gap,ec}}$ [V] ^[a]	Ref.
	1st	2nd	3rd	4th			
$\text{TbNC}@C_{2v}(19138)-C_{76}$	−0.91	−1.26	−1.78	−2.19	0.45	1.36	This work
$\text{YNC}@C_{2v}(19138)-C_{76}$	−0.93	−1.31	−1.81	−2.23	0.46	1.39	This work
$\text{TbNC}@C_2(5)-C_{82}$	−0.88	−0.97	−1.55	−1.91	0.50	1.38	[10c]
$\text{TbNC}@C_s(6)-C_{82}$	−0.59	−0.84	−1.77	−1.92	0.55	1.14	[10a]
$\text{TbNC}@C_{2v}(9)-C_{82}$	−0.46	−0.81	−1.78	−1.96	0.55	1.07	[10a]
$\text{YNC}@C_s(6)-C_{82}$	−0.59	−0.84	−1.76	−1.92	0.56	1.15	[10b]
$\text{Sm}@C_{2v}(19138)-C_{76}$	−0.69	−1.04	−1.62	−1.97	0.32	1.01	[13b]

[a] $\Delta E_{\text{gap,ec}} = E_{1/2,\text{ox}(1)} - E_{1/2,\text{red}(1)}$.

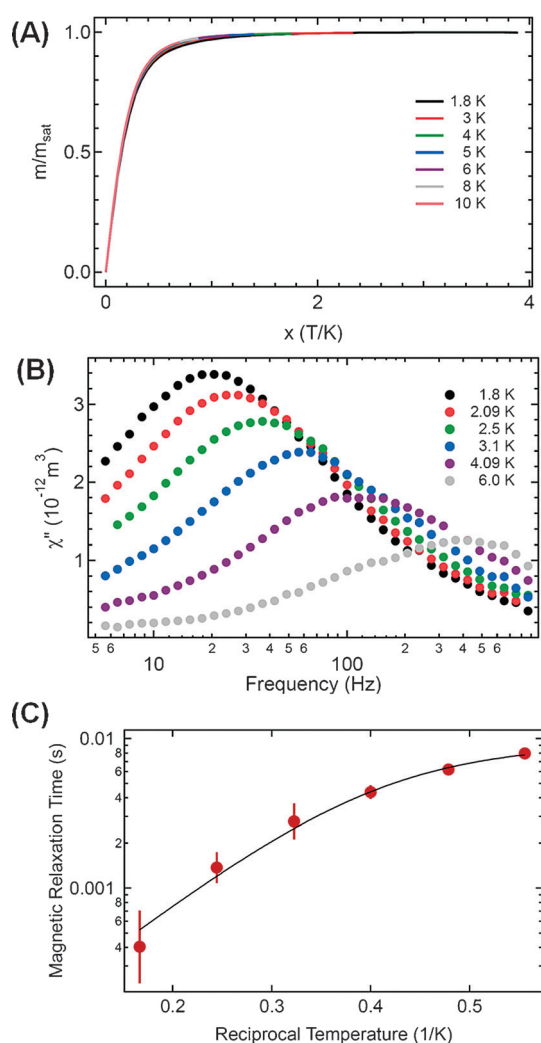


Figure 3. A) Magnetization of TbNC@C_{2v}(19138)-C₇₆ versus the applied field temperature quotient x . The color codes of the different temperatures are indicated. The magnetization curves scale with the applied field temperature quotient $x = \mu_0 H / T$. B) Imaginary part of AC susceptibility measured at different temperatures for TbNC@C_{2v}(19138)-C₇₆. $\mu_0 H = B_0 + B_1 \sin(\omega t)$, $B_0 = 200$ mT, $B_1 = 0.25$ mT. C) Magnetic relaxation times (τ) determined from the data in (B) as a function of reciprocal temperature. The solid line is a 3-parameter fit using the similar function applied for DySc₂N@C₈₀ in Ref. [9a], resulting in the thermal barrier (Δ_{eff}/k_B) of 12 ± 2 K, a prefactor (τ_0) of 80 ± 40 μs and a temperature independent lifetime (τ_c) of 9 ± 1 ms.

Similar to the case of HoSc₂N@C₈₀,^[9d] the AC susceptibility shown in Figure 3B qualifies TbNC@C₇₆ as a field-induced SMM or more specifically single-ion magnet (SIM) which is a SMM containing only one single magnetic ion.^[8b,10a] In low fields ($\mu_0 H = 0.2$ T), the AC susceptibility shows significant temperature dependence of the magnetic relaxation times. Figure 3C shows an Arrhenius plot of the magnetization lifetimes in an applied field $\mu_0 H = 0.2$ T with a fit^[9a] extracting characteristic kinetic parameters for the demagnetization of the observed super-paramagnetism. Above 4 K, a thermal de-magnetization barrier (Δ_{eff}/k_B) of 12 ± 2 K with a prefactor (τ_0) of 80 ± 40 μs can be obtained. At lower temperatures, the magnetic relaxation time saturates where

the fit indicates a maximum lifetime (τ_c) of 9 ± 1 ms for the temperature independent decay of the magnetization (see Supporting Information S7).

In summary, two novel non-IPR mononuclear clusterfullerenes MNC@C₇₆ (M = Tb, Y) have been successfully synthesized and isolated, featuring the stabilization of one pair of fused-pentagons by a mononuclear MNC cluster. The MNC cluster entrapped within the non-IPR C_{2v}(19138)-C₇₆ cage is found to take a nearly linear configuration, which is remarkably different from the triangular geometry of the MNC cluster for the reported IPR-obeying C₈₂ cage-based mononuclear cyanide clusterfullerenes. TbNC@C_{2v}(19138)-C₇₆ and YNC@C_{2v}(19138)-C₇₆ exhibit almost identical electronic properties as shown by UV/Vis-NIR spectroscopic and cyclic voltammetric studies. TbNC@C₇₆ is identified to be a field-induced SMM with a maximum lifetime of 9 ± 1 ms. Our study on the novel non-IPR mononuclear clusterfullerenes provides new insights into the exceptional stabilities of strained fullerene molecules.

Acknowledgements

We thank Profs. L.-S. Zheng and J. Tao (Xiamen University, China) for valuable discussions. This work was partially supported by the National Natural Science Foundation of China (NNSFC, Nos. 21132007, 21371164, 2151101074, 51572254) [to S.F.Y.], the 973 project (2014CB845601) and the NNSFC (no. U1205111, 21390390, 51572231) [to S.Y.X.], DFG (grant PO 1602/1-2 and DU225/31-1), and the European Research Council (ERC) under the European Union's Horizon 2020 research and innovation programme (grant agreement No 648295 "Gram3") [to A.A.P.], and the Swiss National Science Foundation (200021L_147201) within the DACH program [to T.G.]. Computational resources were provided by the Center for Information Services and High Performance Computing (ZIH) in TU Dresden. We thank Ulrike Nitzsche for technical assistance with computational resources in IFW Dresden.

Conflict of interest

The authors declare no conflict of interest.

Keywords: clusterfullerenes · cyanide compounds · endohedral fullerenes · non-IPR carbon cage · single-molecule magnets

How to cite: *Angew. Chem. Int. Ed.* **2017**, *56*, 1830–1834
Angew. Chem. **2017**, *129*, 1856–1860

- [1] A. Hirsch, M. Brettreich, *Fullerenes: Chemistry and Reactions*, Wiley-VCH, Weinheim, **2005**.
- [2] a) P. W. Fowler, D. E. Manolopoulos, *An Atlas of Fullerenes*, Oxford Press, Clarendon, **1995**; b) "Carbon: Fullerenes": F. P. Liu, S. F. Yang, in *Encyclopedia of Inorganic and Bioinorganic Chemistry* (Eds.: C. M. Lukehart, R. A. Scott), Wiley, Hoboken, **2014**, DOI: 10.1002/9781119951438.eibc0033.pub2.
- [3] H. W. Kroto, *Nature* **1987**, *329*, 529–531.

- [4] Y. Z. Tan, S. Y. Xie, R. B. Huang, L. S. Zheng, *Nat. Chem.* **2009**, *1*, 450–460.
- [5] a) A. A. Popov, S. F. Yang, L. Dunsch, *Chem. Rev.* **2013**, *113*, 5989–6113; b) T. S. Wang, C. R. Wang, *Acc. Chem. Res.* **2014**, *47*, 450–458; c) X. Lu, L. Feng, T. Akasaka, S. Nagase, *Chem. Soc. Rev.* **2012**, *41*, 7723–7760; d) A. Rodríguez-Fortea, A. L. Balch, J. M. Poblet, *Chem. Soc. Rev.* **2011**, *40*, 3551–3563; e) M. N. Chaur, F. Melin, A. L. Ortiz, L. Echegoyen, *Angew. Chem. Int. Ed.* **2009**, *48*, 7514–7538; *Angew. Chem.* **2009**, *121*, 7650–7675.
- [6] a) S. Stevenson, P. W. Fowler, T. Heine, J. C. Duchamp, G. Rice, T. Glass, K. Harich, E. Hajdu, R. Bible, H. C. Dorn, *Nature* **2000**, *408*, 427–428; b) M. M. Olmstead, H. M. Lee, J. C. Duchamp, S. Stevenson, D. Marciu, H. C. Dorn, A. L. Balch, *Angew. Chem. Int. Ed.* **2003**, *42*, 900–903; *Angew. Chem.* **2003**, *115*, 928–931; c) M. M. Beavers, M. N. Chaur, M. M. Olmstead, L. Echegoyen, A. L. Balch, *J. Am. Chem. Soc.* **2009**, *131*, 11519–11524; d) B. O. Mercado, C. M. Beavers, M. M. Olmstead, M. N. Chaur, K. Walker, B. C. Holloway, L. Echegoyen, A. L. Balch, *J. Am. Chem. Soc.* **2008**, *130*, 7854–7855; e) T. Zuo, K. Walker, M. M. Olmstead, F. Melin, B. C. Holloway, L. Echegoyen, H. C. Dorn, M. N. Chaur, C. J. Chancellor, C. M. Beavers, A. L. Balch, A. J. Athans, *Chem. Commun.* **2008**, 1067–1069; f) Y. Zhang, K. B. Ghiassi, Q. Deng, N. A. Samoylova, M. M. Olmstead, A. L. Balch, A. A. Popov, *Angew. Chem. Int. Ed.* **2015**, *54*, 495–499; *Angew. Chem.* **2015**, *127*, 505–509; g) N. Chen, C. M. Beavers, M. M. Mulet-Gas, A. Rodríguez-Fortea, E. J. Munoz, Y.-Y. Li, M. M. Olmstead, A. L. Balch, J. M. Poblet, L. Echegoyen, *J. Am. Chem. Soc.* **2012**, *134*, 7851–7860.
- [7] S. F. Yang, F. P. Liu, C. B. Chen, M. Z. Jiao, T. Wei, *Chem. Commun.* **2011**, *47*, 11822–11839.
- [8] a) D. N. Woodruff, R. E. P. Winpenny, R. A. Layfield, *Chem. Rev.* **2013**, *113*, 5110–5148; b) J. Dreiser, *J. Phys. Condens. Matter* **2015**, *27*, 183203.
- [9] a) R. Westerström, J. Dreiser, C. Piamonteze, M. Muntwiler, S. Weyeneth, H. Brune, S. Rusponi, F. Nolting, A. A. Popov, S. F. Yang, L. Dunsch, T. Greber, *J. Am. Chem. Soc.* **2012**, *134*, 9840–9843; b) R. Westerström, J. Dreiser, C. Piamonteze, M. Muntwiler, S. Weyeneth, K. Kramer, S. X. Liu, S. Decurtins, A. A. Popov, S. F. Yang, L. Dunsch, T. Greber, *Phys. Rev. B* **2014**, *89*, 060406; c) R. Westerström, A. C. Uldry, R. Stania, J. Dreiser, C. Piamonteze, M. Muntwiler, F. Matsui, S. Rusponi, H. Brune, S. F. Yang, A. A. Popov, B. Buchner, B. Delley, T. Greber, *Phys. Rev. Lett.* **2015**, *114*, 087201; d) J. Dreiser, R. Westerström, Y. Zhang, A. A. Popov, L. Dunsch, K. Kramer, S. X. Liu, S. Decurtins, T. Greber, *Chem. Eur. J.* **2014**, *20*, 13536–13540; e) K. Junghans, C. Schlesier, A. Kostanyan, N. A. Samoylova, Q. M. Deng, M. Rosenkranz, S. Schiemenz, R. Westerström, T. Greber, B. Büchner, A. A. Popov, *Angew. Chem. Int. Ed.* **2015**, *54*, 13411–13415; *Angew. Chem.* **2015**, *127*, 13609–13613.
- [10] a) F. P. Liu, C.-L. Gao, Q. M. Deng, X. J. Zhu, A. Kostanyan, R. Westerström, S. Wang, Y.-Z. Tan, J. Tao, S.-Y. Xie, A. A. Popov, T. Greber, S. F. Yang, *J. Am. Chem. Soc.* **2016**, *138*, 14764–14771; b) S. F. Yang, C. B. Chen, F. P. Liu, Y. P. Xie, F. Y. Li, M. Z. Jiao, M. Suzuki, T. Wei, S. Wang, X. Lu, Z. F. Chen, T. Akasaka, *Sci. Rep.* **2013**, *3*, 1487; c) F. P. Liu, S. Wang, J. Guan, T. Wei, M. X. Zeng, S. F. Yang, *Inorg. Chem.* **2014**, *53*, 5201–5205.
- [11] a) M. M. Olmstead, C. M. Beavers, A. L. Balch, G. Wang, G. T. Yee, C. Y. Shu, L. Xu, B. Elliott, L. Echegoyen, J. C. Duchamp, H. C. Dorn, *Inorg. Chem.* **2008**, *47*, 5234–5244; b) T. Wei, S. Wang, F. P. Liu, Y. Z. Tan, X. J. Zhu, S. Y. Xie, S. F. Yang, *J. Am. Chem. Soc.* **2015**, *137*, 3119–3123; c) T. Wei, S. Wang, X. Lu, J. Huang, F. P. Liu, Q. X. Li, S. Y. Xie, S. F. Yang, *J. Am. Chem. Soc.* **2016**, *138*, 207–214; d) T. M. Zuo, L. Xu, C. M. Beavers, M. M. Olmstead, W. Fu, T. D. Crawford, A. L. Balch, H. C. Dorn, *J. Am. Chem. Soc.* **2008**, *130*, 12992–12997.
- [12] a) K. J. Harris, R. E. Wasylshen, *Inorg. Chem.* **2009**, *48*, 2316–2332; b) P. A. Stevens, R. J. Madix, J. Stohr, *J. Chem. Phys.* **1989**, *91*, 4338–4345; c) A. G. Orpen, L. Brammer, F. H. Allen, O. Kennard, D. G. Watson, R. J. Taylor, *J. Chem. Soc. Dalton Trans.* **1989**, S1–S83.
- [13] a) X. Lu, Z. Slanina, T. Akasaka, T. Tsuchiya, N. Mizorogi, S. Nagase, *J. Am. Chem. Soc.* **2010**, *132*, 5896–5905; b) Y. J. Hao, L. Feng, W. Xu, Z. N. Gu, Z. Hu, Z. J. Shi, Z. Slanina, F. Uhlik, *Inorg. Chem.* **2015**, *54*, 4243–4248.
- [14] CCDC 997467, 1509471, contain the supplementary crystallographic data for this paper. These data can be obtained free of charge from The Cambridge Crystallographic Data Centre via The Cambridge Crystallographic Data Centre.

Manuscript received: November 19, 2016

Final Article published: January 12, 2017